RSC Advances

PAPER

View Article Online
View Journal | View Issue

Cite this: *RSC Adv.*, 2017, **7**, 15102

Preparation and application of Ni(II) ion-imprinted silica gel polymer for selective separation of Ni(II) from aqueous solution

Hongxing He, Qiang Gan and Changgen Feng*

Received 4th January 2017
Accepted 22nd February 2017

DOI: 10.1039/c7ra00101k

rsc.li/rsc-advances

In the present study, a novel Ni(II) ion-imprinted sulfonate functionalized silica gel polymer was prepared with the surface imprinting technique by using nickel(II) as the template ion, grafted silica gel as the support, and 2-acrylamido-2-methyl-1-propanesulfonic acid (AMPS) and ethylene glycol dimethacrylate (EGDMA) as the functional monomer and crosslinker, respectively. The sorbent was characterized by FT-IR, SEM, EDX, TG and BET. Kinetics studies indicated that the adsorption equilibrium was achieved within 12 min and the adsorption kinetics followed the pseudo-second-order rate equation. The adsorption isotherm was well fitted by the Langmuir model. The Ni(II) ion-imprinted silica gel polymer (Ni(II)-IIP) exhibited a higher adsorption capacity and selectivity for Ni(II) in comparison to the non-imprinted silica gel polymer (Ni(II)-NIP). The maximum adsorption capacities of Ni(II)-IIP and Ni(II)-NIP for Ni(II) were 20.30 and 4.87 mg g^{-1}, respectively. The relative selectivity coefficients of the adsorbent for Ni(II) in the presence of Co(II), Cu(II), Zn(II) and Pb(II) were 4.09, 3.62, 5.78 and 5.86, respectively. Reusability studies indicated that the adsorption capacity of the prepared sorbent did not decrease significantly after repeated use six times. The precision of this method was verified and the prepared sorbent can be considered to be a promising sorbent for selective separation of Ni(II) from natural water samples.

1. Introduction

Many industries, such as the electroplating industry, produce toxic wastewaters containing many heavy metals. Nickel(II) has been identified as one of the toxic heavy metals threats to human beings and other creatures.[1] For example, nickel can cause a skin disorder known as nickel-aczema.[2,3] Therefore, separation and removal of toxic Ni(II) from wastewaters has received wide research attention.

Recently, adsorption has been widely utilized to remove heavy metals from aqueous solutions due to its many advantages, such as low-cost, higher removal efficiency, easy handing, and environmental-friendliness.[4,5] There are a lot of materials, including carbon nanocomposites,[6] magnetic nanoparticles (Fe_3O_4),[7] resins,[8] modified silica gel,[9] carbon nanotubes,[10] fibers,[11] membranes,[12] and biosorbents,[13] that have been used as adsorbents to remove Ni(II) from aqueous solutions. However, the poor recognition of specific metal ions limits their applications. Ion imprinting is a powerful technique for the preparation of polymeric materials which have an outstanding recognition ability for the template ion. Ion imprinted polymers (IIPs) were first proposed by Nishide *et al.* in 1976.[14] The preparation process of IIPs can be generally explained as follows: (1) appropriate functional monomers initially form complexes with template ions; (2) functional groups on the monomers are fixed with crosslinker in the process of polymerization; (3) removal of the template ion leaves binding sites that are matched in size, shape and coordination geometry to the template ion.[15] Consequently, IIPs show the outstanding recognition feature for the target ions over other coexisting metal ions. Unfortunately, traditional IIPs prepared by bulk polymerization method usually suffer from weak binding capacity and slow mass transfer because the binding sites are completely embedded in polymer.[16] Surface imprinting technique (SIT) is developed to solve the above problems. The key point of this technique is fixing binding sites onto the support surface, enabling the target metal ions to combine with binding sites more quickly and easily.[17,18] Therefore, surface ion-imprinted polymers not only possess high selectivity and adsorption capacity, but also have a faster mass transfer and binding kinetics.[19] To date, a lot of Ni(II) ion-imprinted polymers based on biomass have been prepared by surface imprinting technique for removal of nickel(II) from aqueous solution.[20–24] Silica gel has been widely applied as a support for surface imprinting materials due to its low cost, wonderful modification and excellent mechanical stability.[25] However, to our knowledge, there is only one literature on Ni(II) ion surface-imprinted polymer based on silica gel functionalized with

State Key Laboratory of Explosion Science and Technology, Beijing Institute of Technology, Beijing 100081, PR China. E-mail: cgfeng@cast.org.cn; Tel: +86 010 68912941

amino group for selective removal of Ni(II) from aqueous solutions.[19] According to the Lewis theory of acids and bases,[26] Ni(II) belongs to borderline acid and prefers to combine with sulfonic acid ($-SO_3H$) groups which belong to borderline bases.

In the present study, a new Ni(II) ion-imprinted sulfonate functionalized silica gel polymer was prepared with surface imprinting technique by using 2-acrylamido-2-methyl-1-propanesulfonic acid (AMPS) as functional monomer for selective removal of Ni(II) from aqueous solutions. The preparation, characterization, adsorption time, adsorption capacity, selective adsorption and regeneration performance of the prepared polymer were discussed in detail.

2. Experimental

2.1 Materials

2-Acrylamido-2-methyl-1-propanesulfonic acid (AMPS), ethylene glycol dimethacrylate (EGDMA) and 2,2′-azobis(isobutyronitrile) (AIBN) were purchased from Sigma-Aldrich, Milwaukee, USA. Sodium dodecyl sulfate (SDS) was purchased from Sinopharm, Beijing, China. All other reagents were obtained from Beijing Chemical Plant, Beijing, China and all reagents were of analytical grade. All aqueous solutions were prepared using deionized water.

2.2 Apparatus

The pH of the solution was conducted with a PHS-3C pH meter, Shanghai, China. The Fourier transform infrared spectrometry (FT-IR) of all samples were recorded on a Nicolet iS10 IR spectrometer, Waltham, USA. The surface morphology measurements of the imprinted materials were evaluated by a FEG 250 scanning electron microscope, Hillsboro, USA. The thermal stability analysis (TGA) was conducted with a 6300 thermogravimetric analyzer, Tokyo, Japan. Surface areas were determined using NOVA3200e Brunauer–Emmett–Teller (BET) surface area analyzer, Quantachrome, USA. The concentrations of metal ions were determined by a Spectro Arcos inductively coupled plasma atomic emission spectrometry (ICP-AES), Kleve, Germany.

2.3 Real sample preparation

The standard solution of Ni (GBW(E)080128) was purchased from National Institute of Metrology, Beijing, China. The real samples were collected from tap water (the laboratory) and lake water (Beijing, China). All samples were filtered through a 0.22 μm PES membrane and stored in a refrigerator at 4 °C before use. The pH value was adjusted to 7 by 0.1 mol L^{-1} HNO_3 or 0.1 mol L^{-1} $NH_3 \cdot H_2O$ solution.

2.4 Synthesis of Ni(II) ion-imprinted silica gel polymer (Ni(II)-IIP)

2.4.1 Synthesis of *N*-propylmaleamic acid-functionalized silica gel (SG-PMA). SG-PMA was synthesized according to the previous report.[27] Briefly, 5 g SG-AAPTS and 2.5 g maleic anhydride was dispersed in 100 mL of tetrahydrofuran with stirred at room temperature for 24 h. And then, the product was washed with tetrahydrofuran and ethanol successively, finally dried in vacuum at 60 °C for 12 h.

2.4.2 Synthesis of Ni(II) ion-imprinted silica gel polymer (Ni(II)-IIP). The Ni(II) ion-imprinted silica gel polymer (Ni(II)-IIP) was synthesized by surface imprinting technique. Since the functional monomer AMPS is a water-soluble monomer, the polymerization was carried out in emulsion. The procedure was described as follows (Fig. 1).

Firstly, 5.0 g of SDS and 14.5 mL of *n*-pentanol as emulsifiers, 1 mmol of nickel nitrate as template metal ion and 4 mmol of AMPS as monomer were added to 29 mL of toluene with stirring at room temperature. Then, 2 mL of water was added dropwise into the above mixture, the mixture was ultrasonically shaken for 2 min to obtain W/O emulsions. Subsequently, 2.5 g of SG-PMA was added to the emulsions, and the mixture was also stirred for 2 h. Secondly, 1.5 mL of EGDMA as crosslinker and 100 mg of AIBN as initiator were added into the mixture. Then the polymerization mixture was bubbled with N_2 for 30 min to eliminate oxygen before it was sealed. After that, the reaction system was heated at 60 °C for 5 h under magnetic stirring. Finally, the obtained polymers were filtered, washed with methanol, then washed with 2 mol L^{-1} of HNO_3 to leach template ions completely. After complete extraction, the product was washed with deionized water to neutral and dried.

The non-imprinted silica gel polymer (Ni(II)-NIP) was prepared using the same procedure only without the addition of the Ni(II) ion.

2.5 Adsorption experiments

Batch adsorption experiments were used in this study to investigate the adsorption behavior and selectivity of Ni(II)-IIP and Ni(II)-NIP. All adsorption experiments were performed in triplicate. The concentrations of all of metal ions were determined by ICP-AES.

Batch adsorption experiments of the Ni(II)-IIP and Ni(II)-NIP were carried out in a conical flask with cover. To investigated the pH effect on adsorption of Ni(II), 20 mg of sorbent was added to 20 mL of 100 mg L^{-1} Ni(II) solution at varying pH values at 25 °C for 2 h. The pH of the solution was adjusted by 0.1 mol L^{-1} HNO_3 or 0.1 mol L^{-1} $NH_3 \cdot H_2O$ solution. The effect of time on Ni(II) adsorption was measured by adding 50 mg of sorbent into 50 mL of 100 mg L^{-1} Ni(II) solution at different times at 25 °C under the optimum pH conditions. Samples were taken out from the solution at various time intervals until saturation adsorption. To evaluate the static adsorption capacity of the sorbent, 20 mg of sorbent was added to 20 mL of Ni(II) ion solution of varying concentrations (10–150 mg L^{-1}) at 25 °C for 15 min. The adsorption capacity can be calculated by the following equation.

$$q = \frac{c_i - c_f}{1000W} \times V$$

where q (mg g^{-1}) is the adsorption capacity, c_i (mg L^{-1}) and c_f (mg L^{-1}) are the initial and final concentrations of metal ions, respectively, V (mL) is the volume of the solution, and W (g) is the mass used of sorbent.

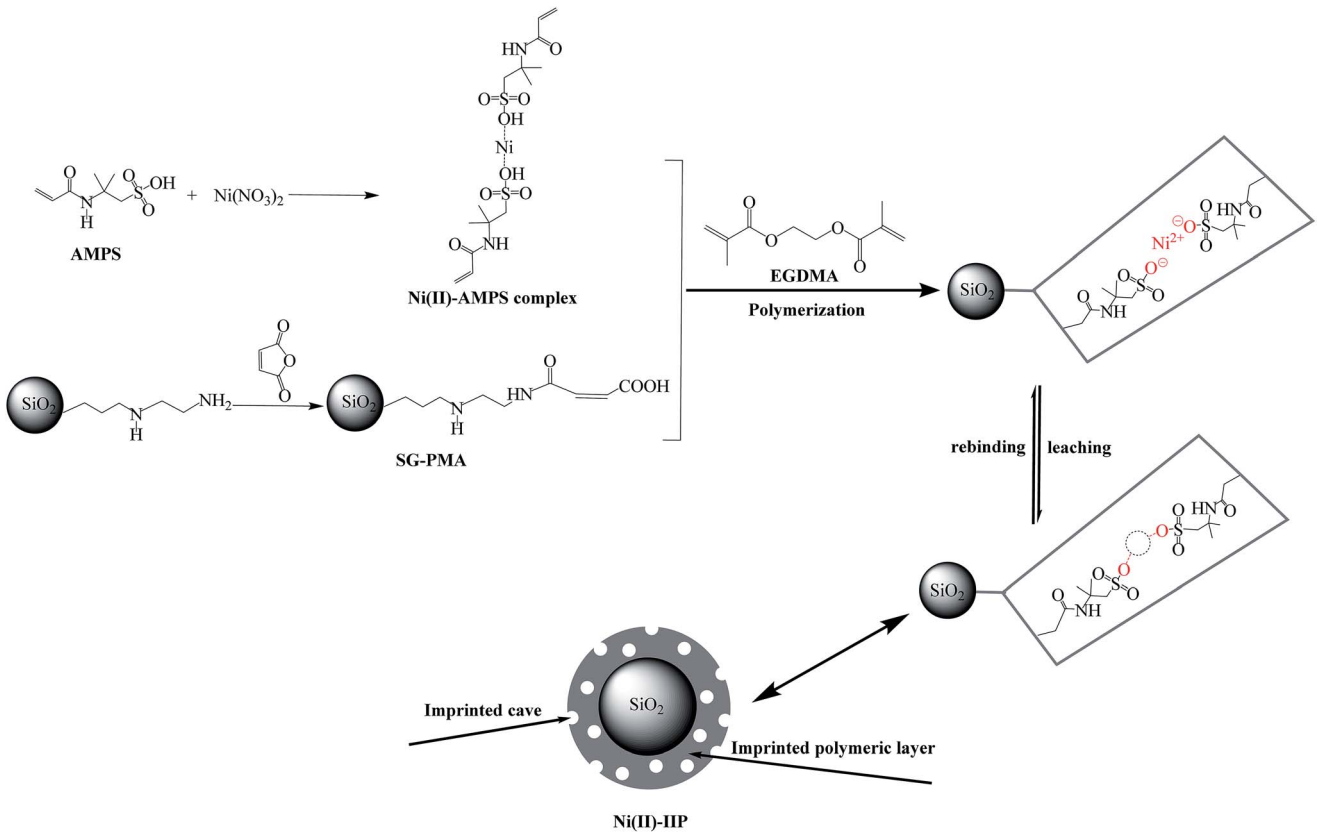

Fig. 1 Scheme for preparation of Ni(II) ion-imprinted polymer.

2.6 Selectivity experiments

To determine the selective adsorption, 10 mg of the sorbent was added into 20 mL of 5 mg L^{-1} binary solutions of Ni(II)/Co(II), Ni(II)/Cu(II), Ni(II)/Zn(II) and Ni(II)/Pb(II) at pH 7.0 for 15 min. The distribution coefficient (D), the selectivity coefficient (k) and the relative selectivity coefficient (k') were calculated according to the following equations.

$$D = \frac{(C_i - C_e)}{C_e} \times \frac{V}{W} \quad k = \frac{D_{Ni}}{D_M} \quad k' = \frac{k_{IIP}}{k_{NIP}}$$

where C_i and C_e are the initial and equilibrium concentrations of metal ions (mg L^{-1}), V is the volume of the solution (mL), and W is the amount of Ni(II)-imprinted polymers (g).

2.7 Reusability studies

To investigate the reusability, adsorption/desorption experiments were reused for six times using the same sorbent. The optimum eluent was investigated by using HNO_3, HCl and H_2SO_4 solutions to desorb the Ni(II) adsorbed on the sorbent. For adsorption experiment, 20 mg of Ni(II)-IIP was equilibrated with 50 mL of 100 mg L^{-1} Ni(II) ion solution at pH 7.0 and 25 °C for 30 min. After adsorption experiments, the sorbent was desorbed by 10 mL of 2 mol L^{-1} HNO_3 solution to leach the Ni(II) ion adsorbed in sorbents completely. After that, the sorbent was filtered and washed with distilled water to neutral, and then dried under vacuum at 50 °C for 12 h before the next adsorption/desorption process.

3. Results and discussions

3.1 Characterizations

3.1.1 FT-IR spectra. Fig. 2 gives the FT-IR spectra of three particles, SG-PMA, Ni(II)-IIP and Ni(II)-NIP. Two sharpness absorption bands at 1099 cm^{-1} and 803 cm^{-1} represent the Si–O–Si and Si–O stretching vibrations, respectively, whereas the absorption peak at 462 cm^{-1} is assigned to bending vibrations of Si–O–Si groups.[28] As compared with the spectrum of SG-PMA, in the spectrum of Ni(II)-IIP and Ni(II)-NIP, two new adsorption band at about 1208 and 1043 cm^{-1} should be ascribed to the asymmetric and symmetric bands of SO_2 in sulfonic acid group from AMPS, the band at around 1659 cm^{-1} is associated to the C–N bond in sulfonic acid, also the band at around 1545 cm^{-1} is assigned to the N–H bond in amide group, along with the band corresponding to the O–H bond in sulfonic acid at 2928 cm^{-1}, indicating the appearance of the functional monomer AMPS.[29] Besides, the band of C–C(=O)–O bond at 1100 cm^{-1} reveals the presence of EGDMA as crosslinker.[30] The results indicated that the polymerization between AMPS and EGDMA took place on silica gel surface and the imprinted layer on the surface of silica gel was formed.

3.1.2 Morphology study. Fig. 3(a) and (b) showed the SEM images of Ni(II)-IIP and Ni(II) loaded Ni(II)-IIP. As can be seen in

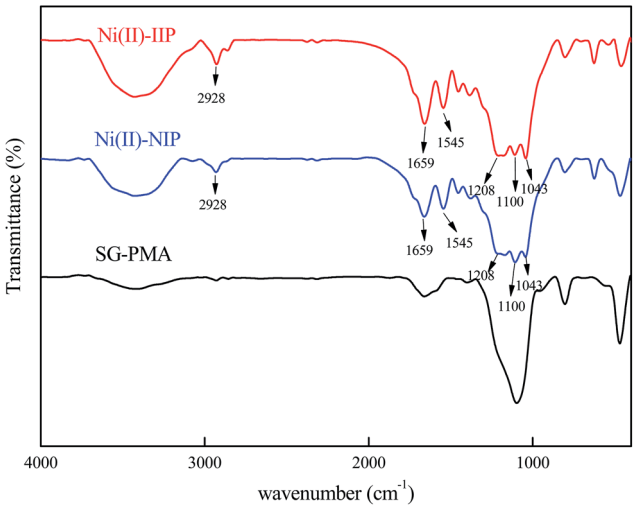

Fig. 2 FT-IR spectra of SG-PMA, Ni(II)-IIP and Ni(II)-NIP.

Fig. 3, some noticeable changes of surface morphology were observed between nickel ions loaded Ni(II)-IIP and Ni(II)-IIP. There are a large number of nanopores on the surface of the Ni(II)-IIP, but after Ni(II) adsorption, some nanopores were filled up. It may be due to the combination of nickel ions with recognition sites on the sorbent surface. The nanopore structure on the imprinted materials surface which serves as the recognition sites plays a major role in the adsorption process, and the specific recognition sites of Ni(II)-IIP can match with Ni(II) ions in size, shape, charge and coordination geometry by ion imprinting. In addition, those differences were proved by EDX spectroscopy. There is no characteristic signal of Ni(II) on the Ni(II)-IIP from Fig. 3(a′), whereas the obvious signal of Ni(II) on the Ni(II) loaded Ni(II)-IIP was observed from Fig. 3(b′). Besides, the obvious signal peak of sulfur element in functional monomer illustrates that the sulfonic acid groups have been polymerized on the silica gel surface.

Table 1 Surface physical parameters of the SG-PMA, Ni(II)-IIP, Ni(II)-NIP and Ni(II)-IIP (loaded)

Sample	Surface area (m^2 g^{-1})	Pore volume (cm^3 g^{-1})	Average pore diameter (nm)
SG-PMA	203.4	0.45	9.6
Ni(II)-IIP	238.6	0.56	4.9
Ni(II)-NIP	216.5	0.47	6.6
Ni(II)-IIP (loaded)	219.0	0.48	4.9

3.1.3 Surface area and pore size analysis. The surface area was determined by the Brunauer–Emmett–Teller (BET) method and the average pore size distributions were analyzed by the Barrett–Joyner–Halenda (BJH) method. The surface areas and porosity data of SG-PMA, Ni(II)-IIP, Ni(II)-NIP and the nickel(II) loaded Ni(II)-IIP were listed in Table 1. It can be observed that the surface area, pore volume and average pore diameter changed after polymerization, this is because the polymer layer with nanoporous was formed on the surface of SG-PMA. The surface area of Ni(II)-IIP was greater than that of Ni(II)-NIP, which could be attributed to the specific recognition cavities for Ni(II) formed on the surface of sorbent by imprinting technique. In addition, the surface area of Ni(II)-IIP changed after Ni(II) adsorption, this is likely owing to the combination of nickel ions with recognition cavities on the polymer surface. This is consistent with the observation of the surface morphology.

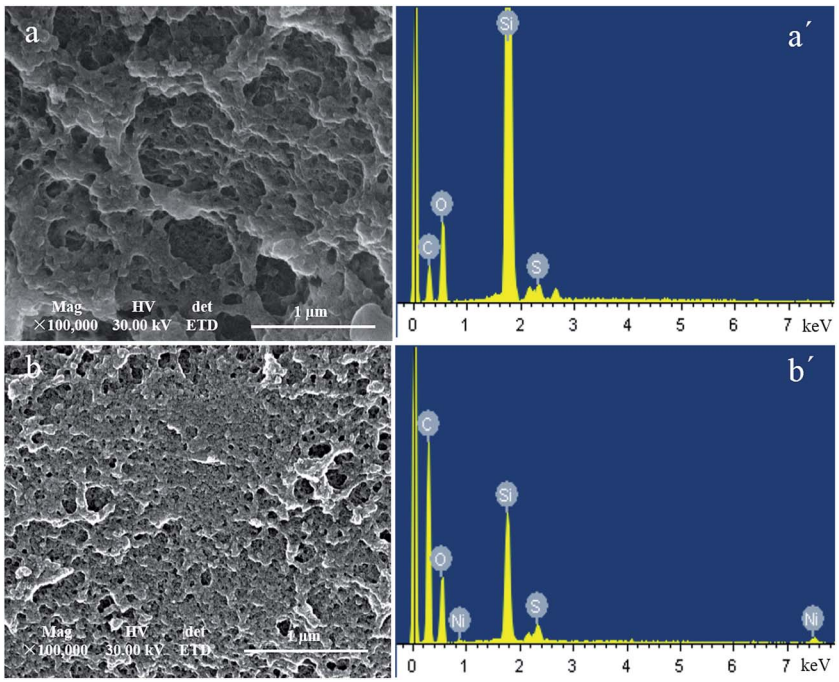

Fig. 3 SEM images of the Ni(II)-IIP (a) and Ni(II) loaded Ni(II)-IIP (b); EDX spectra for the free (a′) and Ni(II)-loaded (b′) Ni(II)-IIP.

3.1.4 Thermal stability. Thermal stability of the prepared Ni(II)-IIP was studied using a thermogravimetric analysis (TG) technique. Fig. 4 represents TG curves of SG-PMA and Ni(II)-IIP. For SG-PMA, when the temperature increased from room temperature to 150 °C, the weight loss was about 5.8%, which mainly owing to the loss of the physically attached water molecules. The weight loss of 18.3% from 150 °C to 800 °C due to the decomposition of the organic compounds grafted on the silica gel surface. For Ni(II)-IIP, the first weight loss was about 4.1% from room temperature to 150 °C, it can be due to the physisorbed water. When the temperature changed from 150 °C to 800 °C, the large weight loss was about 42.8%, which might be assigned to the decomposition of poly(AMPS-*co*-EGDMA) on the silica gel. The results indicated that a polymer layer was coated on the silica gel surface. On the other hand, the results showed that the prepared sorbent had a good thermal stability.

3.2 Adsorption of Ni(II) on Ni(II)-IIP

3.2.1 Effect of pH on adsorption of Ni(II). The pH of the solution is one of the important factors in the whole Ni(II) adsorption process. Considering 100 mg L^{-1} of nickel ions will be hydrolyzed when pH of solution is greater than 8.0, the experiments were conducted at pH = 1.0 to 8.0. Fig. 5 shows the effect of pH of solutions on Ni(II) adsorption. It can be seen that the adsorption capacity of Ni(II) increased rapidly from pH 1.0 to 4.0, then further increased at a slow rate from pH 4.0 to 7.0, finally decreased at pH > 8.0. Below pH 4.0, the cause of low adsorption capacity is mainly the protonation of the sulfonic groups, large amounts of H^+ inhibited the adsorption of the binding sites for Ni(II) in aqueous solution. Over pH 7.0, adsorption capacity decreased probably due to the widespread hydrolysis of Ni(II) ion as expected, which leads to the concentration of free Ni(II) ion in the sample solution decreased. The maximum adsorption capacity (19.06 mg g^{-1}) was obtained at pH 7.0. Therefore, a pH value of 7.0 in aqueous solution was chosen as the optimum pH in the later experiments.

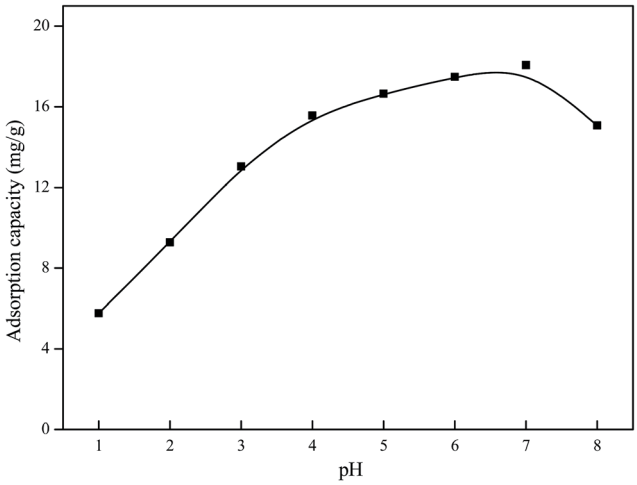

Fig. 5 Effect of pH on the adsorption capacity of Ni(II)-IIP for Ni(II) (Ni(II) concentration: 100 mg L^{-1}, temperature: 25 °C).

3.2.2 Adsorption kinetics. The effect of contact time on the Ni(II) adsorption on Ni(II)-IIP and Ni(II)-NIP was investigated at 25 °C, pH 7.0 and an initial Ni(II) concentration of 100.0 mg L^{-1}. The results are shown in Fig. 6. As can be seen, both sorbents had a fast adsorption rate for Ni(II) at the first 12 min and soon reached the adsorption equilibrium. It can be ascribed to the fact that there are a large number of binding sites on the polymer surface, which reduces the mass transfer resistance of the Ni(II) adsorption and enables Ni(II) to interact readily with the sorbent, therefore sorbents obtain a high adsorption rate.[31] After fast stage, the external binding sites were gradually occupied by Ni(II) and the amount of available binding sites reduced, the diffusion of Ni(II) into the sorbents inside caused the slow adsorption rate.

Moreover, two kinetic models, pseudo-first-order kinetics model and pseudo-second-order kinetics model were applied to investigate the kinetic mechanism of Ni(II)-IIP for Ni(II)

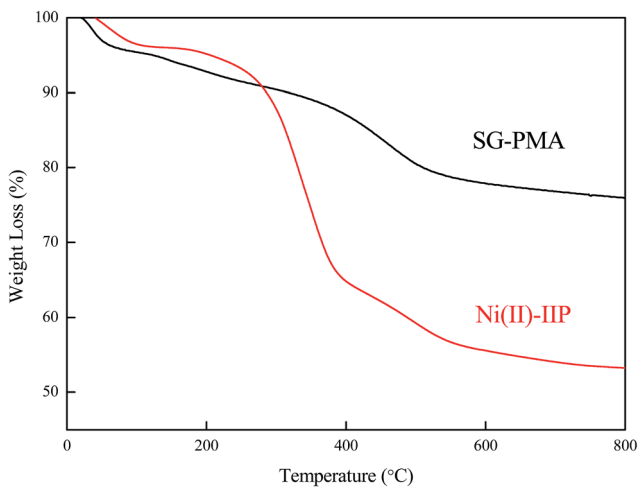

Fig. 4 TG curves of SG-PMA and Ni(II)-IIP.

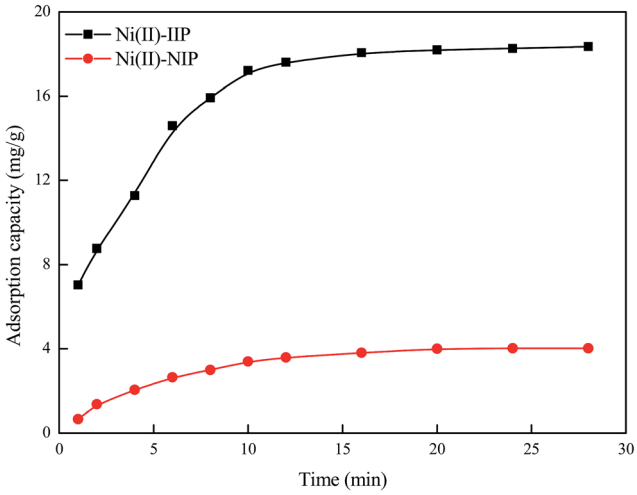

Fig. 6 Effect of contact time on the adsorption of Ni(II)-IIP and Ni(II)-NIP (Ni(II) concentration: 100 mg L^{-1}, pH: 7.0, temperature: 25 °C).

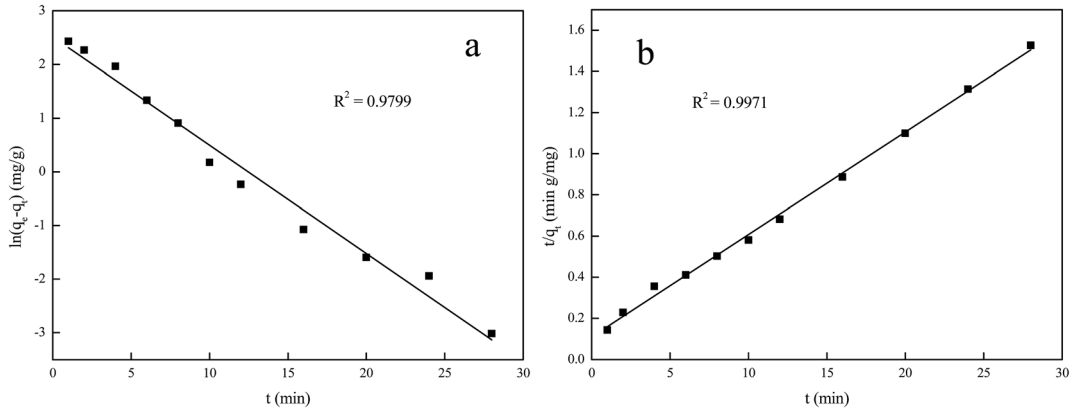

Fig. 7 Pseudo-first-order (a) and pseudo-second-order (b) kinetics of Ni(II)-IIP for adsorption of Ni(II).

adsorption. The linear form of pseudo-first-order kinetics model is expressed as follows:[32]

$$\ln(q_e - q_t) = \ln q_e - k_1 t$$

where q_t (mg g^{-1}) and q_e (mg g^{-1}) are the adsorption capacities of Ni(II) at time t and at equilibrium, respectively. k_1 (min^{-1}) is the rate constant of the first-order model.

The linear form of pseudo-second-order kinetics model is expressed as follows:[32]

$$\frac{t}{q_t} = \frac{1}{k_2 q_e^2} + \frac{1}{q_e} t$$

where k_2 (g min^{-1} mg^{-1}) is the rate constant for pseudo-second-order model at the equilibrium. Likewise, all variables in pseudo-second-order model are as described for pseudo-first-order model.

Fig. 7 presents the plots of pseudo-first-order and pseudo-second-order model for the adsorption nickel(II) and the parameters of the two kinetic models are given in Table 2. It can be seen that the correlation coefficients for the pseudo-first-order kinetics model ($R_1^2 = 0.9799$) was poor and the calculated values of q_e was not match the experimental value, whereas the correlation coefficients for the pseudo-second-order model ($R_2^2 = 0.9971$) was greater than 0.99 and the calculated values of q_e was close to the experimental value. The pseudo-first-order kinetics model assumes that the adsorption process is carried out by the diffusion of metal ions through the boundary layer of the sorbent surface and this adsorption process is controlled by diffusion step, while the pseudo-second-order model considers that the adsorption process is controlled by the chemical adsorption mechanism, which involves the electron sharing or electron transfer between adsorbent and adsorbate. The results suggested that the pseudo-second-order model could better describe the adsorption process of Ni(II) on Ni(II)-IIP and the chemisorption could be the rate-limiting step for Ni(II) adsorption on Ni(II) ion-imprinted polymer.[33]

3.2.3 Maximum adsorption capacity and adsorption isotherm. In order to study the maximum adsorption capacity, the effect of Ni(II) initial concentrations on adsorption of Ni(II)-IIP and Ni(II)-NIP was investigated at 25 °C and pH 7.0 with the initial Ni(II) concentration in the range of 10–150 mg L^{-1}. As shown in Fig. 8, the adsorption capacity of Ni(II) on the imprinted sorbent increased with increasing initial Ni(II)

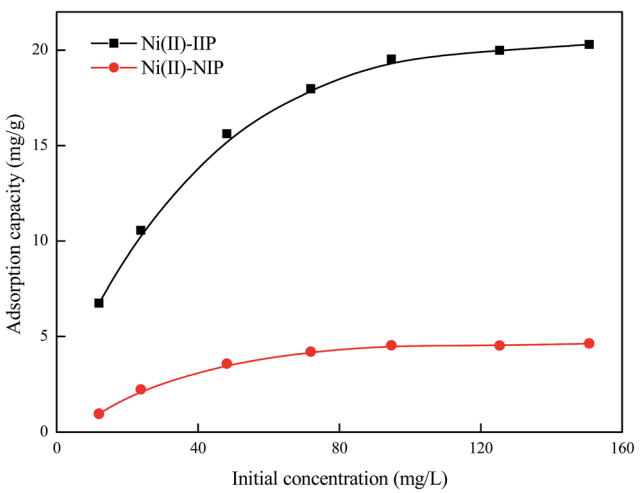

Fig. 8 Effect of Ni(II) initial concentration on the adsorption of Ni(II)-IIP and Ni(II)-NIP (pH: 7.0, temperature: 25 °C).

Table 2 Adsorption kinetic parameters of Ni(II)-IIP for Ni(II) adsorption

	Pseudo-first-order rate equation			Pseudo-second-order rate equation		
$q_{e,exp}$ (mg g^{-1})	k_1 (min^{-1})	$q_{e,cal}$ (mg g^{-1})	R_1^2	k_2 (mg g^{-1} min^{-1})	$q_{e,cal}$ (mg g^{-1})	R_2^2
18.35	0.2018	12.34	0.9799	0.0228	20.07	0.9971

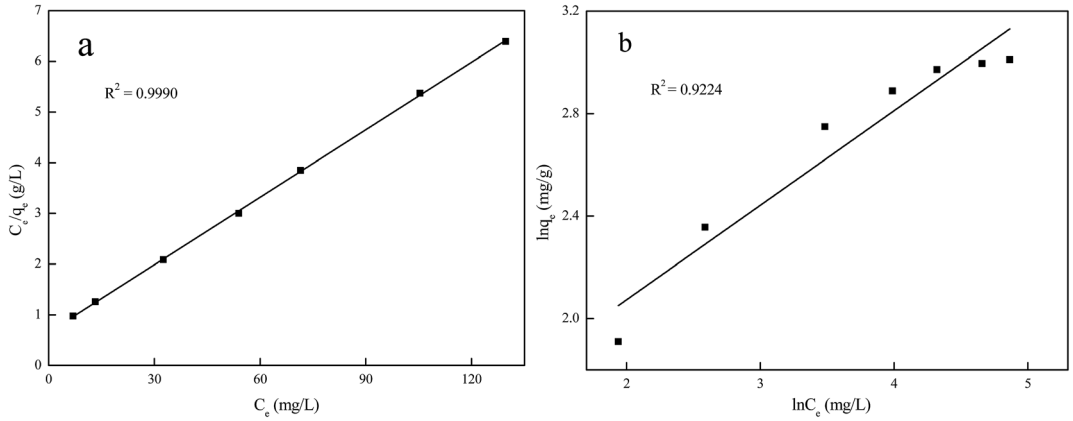

Fig. 9 Langmuir (a) and Freundlich (b) isotherm models of Ni(II)-IIP for Ni(II) adsorption.

concentration, then the adsorption reached saturation after the concentration of 100 mg L^{-1}, and the maximum adsorption capacities of Ni(II) on Ni(II)-IIP and Ni(II)-NIP were 20.30 mg g^{-1} and 4.87 mg g^{-1}, respectively. The maximum adsorption capacity of Ni(II)-IIP was as much as 4.2 times that of Ni(II)-NIP, which indicates that ion imprinting process can greatly enhance the adsorption ability of Ni(II) ion-imprinted polymer. In the published literature,[19] the maximum adsorption capacity of imprinted silica gel adsorbent for Ni(II) was 12.61 mg g^{-1}, it suggested that Ni(II)-IIP prepared in this work had a high adsorption capacity for Ni(II).

In addition, the data of the adsorption equilibrium of Ni(II) on Ni(II)-IIP were fitted to the Langmuir and Freundlich isotherm models. Langmuir and Freundlich isotherm models, which assume a monolayer adsorption on a homogenous surface or sorption on a heterogeneous surface, respectively. The linear expressions of two models were as follows.[34]

Langmuir isotherm:

$$\frac{c_e}{q_e} = \frac{K}{q_m} + \frac{c_e}{q_e}$$

Freundlich isotherm:

$$\ln q_e = \frac{1}{n}\ln c_e + \ln K_F$$

where q_e (mg g^{-1}) is the adsorption capacity of Ni(II) at equilibrium, c_e (mg L^{-1}) is the equilibrium concentration of Ni(II) in the solution, q_m (mg g^{-1}) is the maximal adsorption capacity of Ni(II), K (L g^{-1}) is a constant in the Langmuir model. K_F and n are the constants in the Freundlich model.

Table 3 Adsorption isotherm parameters of Ni(II)-IIP for Ni(II) adsorption

Langmuir adsorption isotherm	Freundlich adsorption isotherm
$q_m = 22.53$ mg g^{-1}	$K_F = 3.80$ mg g^{-1}
$K = 14.77$ L g^{-1}	$n = 2.71$
$R^2 = 0.9990$	$R^2 = 0.9224$

The plots of Langmuir and Freundlich isotherm models are presented in Fig. 9 and the parameters of two isotherm models are given in Table 3. The results showed that the correlation coefficients of the Langmuir model ($R^2 = 0.9990$) was closer to 1 than that of the Freundlich model ($R^2 = 0.9224$). Moreover, the calculation value of the maximal adsorption capacity (22.53 mg g^{-1}) from the Langmuir model was very close to the experimental value (20.30 mg g^{-1}). Therefore, Langmuir model was suitable to depict the adsorption isotherm of Ni(II) on Ni(II)-IIP, that is to say, the adsorption of Ni(II) on Ni(II)-IIP is a monolayer adsorption on the surface of the sorbent.[35]

3.3 Adsorption selectivity

To assess the selectivity of Ni(II)-IIP and Ni(II)-NIP, the selective adsorption experiments were conducted by selecting Co(II), Cu(II), Zn(II) and Pb(II) as competitive ions because they have the same charge and similar size and coexist in natural sources. The data of the distribution coefficient (D), the selectivity coefficient (k) of Ni(II) with respect to other competitive ions and relative selectivity coefficients (k') are listed in Table 4. As shown in Table 4, D values of Ni(II)-IIP for Ni(II) were greater than those of Ni(II)-NIP, besides the Ni(II)-IIP exhibited much greater k value for Ni(II) than other competitive ions. Furthermore, k' values for Ni(II)/Co(II), Ni(II)/Cu(II), Ni(II)/Zn(II) and Ni(II)/Pb(II) were 4.09, 3.62, 5.78 and 5.86, respectively, which was greater than 1. The results revealed that Ni(II)-IIP had high selectivity for Ni(II) in binary systems. As is known to all, based on the hard–soft acid–base theory, sulfonic acid functional group (–SO_3H) belongs to borderline base, which can form complex with borderline acid more readily than hard or soft acids. In this study, although Ni(II), Co(II), Cu(II), Zn(II) and Pb(II) are all of borderline acids, Ni(II)-IIP still has strong selective adsorption of nickel(II) in the presence of other interfering ions. This may be the following two reasons. First, it may be the cavity size selectivity. The ionic radius of Ni(II), Co(II), Cu(II), Zn(II) and Pb(II) are 0.069, 0.065, 0.073, 0.074 and 0.119 Å, respectively. Cu(II), Zn(II) and Pb(II) with greater size than Ni(II) can not enter the imprinted cavities of Ni(II)-IIP, while Co(II) with smaller size do not match the imprinted cavity. Second, it could be

Table 4 Selectivity parameters of Ni(II)-IIP and Ni(II)-NIP

Binary system	Distribution ratio D (mL g^{-1})			Selectivity coefficient k	Relative selective coefficient k'
	Sorbent	D (Ni)	D (M)		
Ni(II)/Co(II)	Ni(II)-IIP	2705.29	585.02	4.62	4.09
	Ni(II)-NIP	286.04	254.30	1.13	
Ni(II)/Cu(II)	Ni(II)-IIP	2479.56	705.78	3.51	3.62
	Ni(II)-NIP	265.09	274.65	0.97	
Ni(II)/Zn(II)	Ni(II)-IIP	3218.25	535.67	6.01	5.78
	Ni(II)-NIP	297.84	287.51	1.04	
Ni(II)/Pb(II)	Ni(II)-IIP	3245.09	485.90	6.68	5.86
	Ni(II)-NIP	309.21	272.24	1.14	

attributed to the coordination geometry selectivity. Ni(II)-IIP can provide the functional groups which coordinate with Ni(II) in a specific geometric space structure, accordingly, despite many metal ions which belong to borderline acid in this work have high affinity with sulfonic acid groups, the sorbent still exhibits high selectivity for Ni(II). The results indicated that coordination geometry selectivity may be the main reason in the selective adsorption process.

3.4 Desorption and reusability

The reusability of the sorbent is one of the most important parameters for its practical application. Desorption experiments of the Ni(II) loaded Ni(II)-IIP were also conducted by a batch method. In order to find a suitable eluent, three kinds of eluents, HCl (0.5 mol L^{-1}), H_2SO_4 (0.5 mol L^{-1}), and HNO_3 (0.5 mol L^{-1}, 1.0 mol L^{-1} and 2.0 mol L^{-1}) solutions were used for desorption experiments. HNO_3 solution was found to be the most effective eluent to remove the adsorbed Ni(II), and a high recovery (99.2%) was obtained when the concentration of eluent was up to 2.0 mol L^{-1}. It can be explained that the nitrogen and oxygen atoms used as donors strengthened the protonation of the sulfonic acid group. Consequently, 10 mL of 2 mol L^{-1} HNO_3 solution was selected as an eluent to desorb Ni(II) adsorbed on the sorbent.

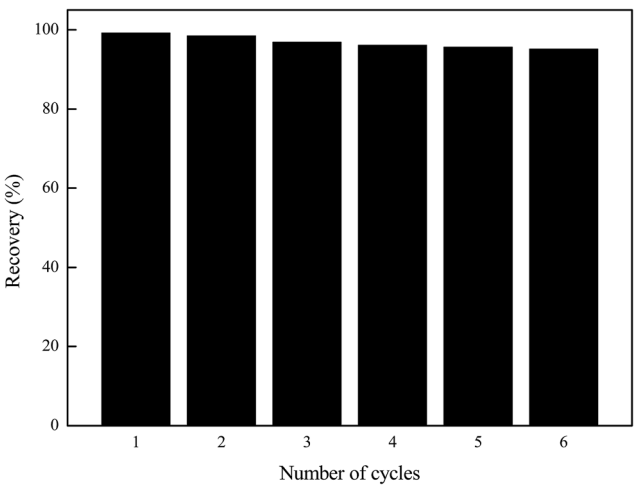

Fig. 10 Desorption and reusability of Ni(II)-IIP.

To study the reusability of the prepared Ni(II) ion-imprinted polymer, the adsorption–desorption cycle of Ni(II) on the Ni(II)-IIP was repeated six times and the results are shown in Fig. 10. It can be seen that the recovery of Ni(II)-IIP for Ni(II) was only 4.9% lower after six adsorption/desorption cycles. The results showed that the prepared Ni(II) ion-imprinted polymer had excellent reusability for Ni(II) adsorption.

3.5 Analytical performance and real sample analysis

In order to assess the analytical precision of the proposed method, under the selected conditions in this study, six portions of standard solutions of Ni(II) (GBW(E)080128, 100 μg L^{-1}) were adsorbed and determinated. The Ni(II) concentration of the proposed method was calculated to be 99.78 ± 2.64 μg L^{-1}, which was in good agreement with the certified value, the relative standard deviation (RSD, %) of the method was 2.65%. The results indicated that the proposed method was suitable for analyzing Ni(II) in aqueous solution.

The proposed method was used for the analysis of Ni(II) in natural water samples by using standard addition method. As is shown in Table 5, the recovery of Ni(II) ions was over 98%, which indicated that the proposed method was suitable for selective separation of Ni(II) from natural water.

3.6 Comparison with other Ni(II) imprinted sorbents

The adsorption properties of Ni(II)-IIP for Ni(II) ion was compared with other Ni(II) imprinted sorbents reported in the literature listed in Table 6. It can be seen Ni(II)-IIP exhibits higher adsorption capacity and good selectivity. In addition, the shorter adsorption time (less than 12 min) and the stability of Ni(II)-IIP for Ni(II) ion are other advantages in comparison to some other sorbents for the removal of Ni(II) ion. Therefore, the

Table 5 Analysis of Ni(II) in real water samples

Samples	Added (μg L^{-1})	Found (μg L^{-1})	Recovery (%)
Tap water	0	0.68 ± 0.04	—
	5	5.57 ± 0.03	98.15
	10	10.53 ± 0.04	98.61
Lake water	0	1.63 ± 0.03	—
	5	6.58 ± 0.02	99.26
	10	11.56 ± 0.04	99.43

Table 6 Comparison of adsorption properties of some surface-imprinted sorbent for Ni(II) ion

Functional monomers	Adsorption capacity (mg g^{-1})	Relative selective coefficient	References
3-Aminopropyltrimethoxysilane	12.61	32.83[a], 45.99[b], 43.79[c], 28.36[d]	19
Vinylbenzyl iminodiacetic acid	12.00	—	36
1,5-Diphenylcarbazide	40.29	17.6[a], 5.9[b], 18.8[c], 20.6[d]	37
1-(Pyridin-2-yl)-*N*-(3-vinylbenzyl) methanamine	11.74	4.8[c]	38
Chitosan	38.49	—	22
2-Acrylamido-2-methyl-1-propanesulfonic acid	20.30	4.09[a], 3.62[b], 5.78[c], 5.86[d]	This work

[a] Ni^{2+}/Co^{2+}. [b] Ni^{2+}/Cu^{2+}. [c] Ni^{2+}/Zn^{2+}. [d] Ni^{2+}/Pb^{2+}.

results indicated that the prepared Ni(II) surface-imprinted gel polymer is a promising candidate for the removal of Ni(II) ion from aqueous solution.

4. Conclusion

In the present study, a new Ni(II) surface-imprinted sulfonate functionalized silica gel sorbent was synthesized by surface imprinting technique. The obtained Ni(II)-IIP was used to investigate adsorption of Ni(II) from aqueous solution. The results showed that the prepared surface imprinted polymer had fast adsorption rate, high adsorption capacity and good selectivity towards Ni(II) at an optimum pH 7 due to the recognition cavities of Ni(II)-IIP highly matched with Ni(II) in size, shape and coordination geometry. The adsorption kinetics of the sorbent followed the pseudo-second-order rate equation and the adsorption isotherm was well fitted by the Langmuir model. The sorbent can be reused for many times without significantly reducing its adsorption capacity. The proposed method was suitable for analyzing Ni(II) in aqueous solution. It can be concluded that the synthesized Ni(II) surface-imprinted silica gel sorbent is a promising sorbent for selective separation of Ni(II) from natural water.

References

1 E. Denkhaus and K. Salnikow, Nickel essentiality, toxicity, and carcinogenicity, *Crit. Rev. Oncol. Hematol.*, 2002, **42**, 35–56.
2 J. Kristiansen, J. M. Christensen, T. Henriksen, N. H. Nielsen and T. Menne, Determination of nickel in fingernails and forearm skin (stratum corneum), *Anal. Chim. Acta*, 2000, **403**, 265–272.
3 A. E. Martell and R. D. Hancock, *Metal Complexes in Aqueous Solutions*, Plenum Press, New York, 1996, ch. 5, p. 160.
4 A. Demirbas, Heavy metal adsorption onto agro-based waste materials: a review, *J. Hazard. Mater.*, 2008, **157**, 220–229.
5 A. S. Özcan, Ö. Gök and A. Özcan, Adsorption of lead(II) ions onto 8-hydroxy quinoline-immobilized bentonite, *J. Hazard. Mater.*, 2009, **161**, 499–509.
6 L. Chen, T. Ji, L. Mu, Y. Shi, L. Brisbin, Z. Guo, M. A. Khan, D. P. Young and J. Zhu, Facile synthesis of mesoporous carbon nanocomposites from natural biomass for efficient dye adsorption and selective heavy metal removal, *RSC Adv.*, 2016, **6**, 2259–2269.
7 P. Panneerselvam, N. Morad and K. A. Tan, Magnetic nanoparticle (Fe_3O_4) impregnated onto tea waste for the removal of nickel(II) from aqueous solution, *J. Hazard. Mater.*, 2011, **186**, 160–168.
8 A. H. Elshazly and A. H. Konsowa, Removal of nickel ions from wastewater using a cation-exchange resin in a batch-stirred tank reactor, *Desalination*, 2003, **158**, 189–193.
9 N. Tokman, S. Akman and M. Ozcan, Solid-phase extraction of bismuth, lead and nickel from seawater using silica gel modified with 3-aminopropyltriethoxysilane filled in a syringe prior to their determination by graphite furnace atomic absorption spectrometry, *Talanta*, 2003, **59**, 201–205.
10 M. I. Kandah and J. L. Meunier, Removal of nickel ions from water by multi-walled carbon nanotubes, *J. Hazard. Mater.*, 2007, **146**, 283–288.
11 F. Ji, C. Li, B. Tang, J. Xu, G. Lu and P. Liu, Preparation of cellulose acetate/zeolite composite fiber and its adsorption behavior for heavy metal ions in aqueous solution, *Chem. Eng. J.*, 2012, **209**, 325–333.
12 E. Katsou, S. Malamis, K. J. Haralambous and M. Loizidou, Use of ultrafiltration membranes and aluminosilicate minerals for nickel removal from industrial wastewater, *J. Membr. Sci.*, 2010, **360**, 234–249.
13 D. H. K. Reddy, D. K. V. Ramana, K. Seshaiah and A. V. R. Reddy, Biosorption of Ni(II) from aqueous phase by *Moringa oleifera*, bark, a low cost biosorbent, *Desalination*, 2011, **268**, 150–157.
14 H. Nishide, J. Deguchi and E. Tsuchida, Selective adsorption of metal ions on crosslinked poly(vinylpyridine) resin prepared with a metal ion as a template, *Chem. Lett.*, 1976, **5**, 169–174.
15 T. P. Rao, R. Kala and S. Daniel, Metal ion-imprinted polymers-novel materials for selective recognition of inorganics, *Anal. Chim. Acta*, 2006, **578**, 105–116.
16 D. K. Singh and S. Mishra, Synthesis, characterization and analytical applications of Ni(II)-ion imprinted polymer, *Appl. Surf. Sci.*, 2010, **256**, 7632–7637.
17 D. M. Han, G. Z. Fang and X. P. Yan, Preparation and evaluation of a molecularly imprinted sol–gel material for on-line solid-phase extraction coupled with high performance liquid chromatography for the determination of trace pentachlorophenol in water samples, *J. Chromatogr. A*, 2005, **1100**, 131–136.
18 K. Y. Yu, K. Tsukagoshi, M. Maeda and M. Takagi, Metal ion-imprinted microspheres prepared by reorganization of the

coordinating groups on the surface, *Anal. Sci.*, 1992, **8**, 701–703.

19 N. Jiang, X. Chang, H. Zheng, Q. He and Z. Hu, Selective solid-phase extraction of nickel(II) using a surface-imprinted silica gel sorbent, *Anal. Chim. Acta*, 2006, **577**, 225–231.

20 L. Zhang, L. Zhong, S. Yang, D. Liu, Y. Wang, S. Wang, X. Han and X. Zhang, Adsorption of Ni(II) ion on Ni(II) ion-imprinted magnetic chitosan/poly(vinyl alcohol) composite, *Colloid Polym. Sci.*, 2015, **293**, 2497–2506.

21 Q. Li, H. Su, J. Li and T. Tan, Studies of adsorption for heavy metal ions and degradation of methyl orange based on the surface of ion-imprinted adsorbent, *Process Biochem.*, 2007, **42**, 379–383.

22 Q. Li, H. Su, J. Li and T. Tan, Application of surface molecular imprinting adsorbent in expanded bed for the adsorption of Ni^{2+} and adsorption model, *J. Environ. Manage.*, 2007, **85**, 900–907.

23 U. K. Garg, M. P. Kaur, V. K. Garg and D. Sud, Removal of nickel(II) from aqueous solution by adsorption on agricultural waste biomass using a response surface methodological approach, *Bioresour. Technol.*, 2008, **99**, 1325–1331.

24 H. Su, S. Chen and T. Tan, Surface active site model for Ni^{2+} adsorption of the surface imprinted adsorbent, *Process Biochem.*, 2007, **42**, 612–619.

25 A. Timin, E. Rumyantsev and A. Solomonov, Synthesis and application of amino-modified silicas containing albumin as hemoadsorbents for bilirubin adsorption, *J. Non-Cryst. Solids*, 2014, **385**, 81–88.

26 R. G. Pearson, Hard and soft acids and bases, *J. Am. Chem. Soc.*, 1963, **22**, 3533–3539.

27 M. Li, M. Y. Li, C. G. Feng and Q. X. Zeng, Preparation and characterization of multicarboxyl-functionalized silica gel for removal of Cu(II), Cd(II), Ni(II) and Zn(II) from aqueous solution, *Appl. Surf. Sci.*, 2014, **314**, 1063–1069.

28 H. T. Fan, T. Sun, Z. G. Zhang and W. X. Li, Selective removal of lead(II) from aqueous solution by an ion-imprinted silica sorbent functionalized with chelating N-donor atoms, *J. Chem. Eng. Data*, 2014, **59**, 2106–2114.

29 Y. Ge, Y. Li, B. Zu, C. Zhou and X. Dou, AM-DMC-AMPS Multi-functionalized magnetic nanoparticles for efficient purification of complex multiphase water system, *Nanoscale Res. Lett.*, 2016, **11**, 1–9.

30 X. Cai, J. Li, Z. Zhang, F. Yang, R. Dong and L. Chen, Novel Pb^{2+} ion imprinted polymers based on ionic interaction *via* synergy of dual functional monomers for selective solid-phase extraction of Pb^{2+} in water samples, *ACS Appl. Mater. Interfaces*, 2014, **6**, 305–313.

31 J. Wang and X. Li, Ion-Imprinted Composite Hydrogels with Excellent Mechanical Strength for Selective and Fast Removal of Cu^{2+}, *Ind. Eng. Chem. Res.*, 2013, **52**, 572–577.

32 J. H. Chen, H. Lin, Z. H. Luo, Y. S. He and G. P. Li, Cu(II)-imprinted porous film adsorbent Cu-PVA-SA has high uptake capacity for removal of Cu(II) ions from aqueous solution, *Desalination*, 2011, **277**, 265–273.

33 M. Yurdakoc, Y. Scki and S. K. Yuedakoc, Kinetic and thermodynamic studies of boron removal by Siral 5, Siral 40, and Siral 80, *J. Colloid Interface Sci.*, 2005, **286**, 440–446.

34 E. Demirbas, N. Dizge, M. T. Sulak and M. Kobya, Adsorption kinetics and equilibrium of copper from aqueous solutions using hazelnut shell activated carbon, *Chem. Eng. J.*, 2009, **148**, 480–487.

35 Z. Ren, D. Kong, K. Wang and W. Zhang, Preparation and adsorption characteristics of an imprinted polymer for selective removal of Cr(VI) ions from aqueous solutions, *J. Mater. Chem. A*, 2014, **2**, 17952–17961.

36 V. Lenoble, W. Meouche, K. Laatikainen, C. Garnier, H. Brisset, A. Margaillan and C. Branger, Assessment and modelling of Ni(II) retention by an ion-imprinted polymer: application in natural samples, *J. Colloid Interface Sci.*, 2015, **448**, 473–481.

37 S. Abbasi, M. Roushani, H. Khani, R. Sahraei and G. Mansouri, Synthesis and application of ion-imprinted polymer nanoparticles for the determination of nickel ions, *Spectrochim. Acta, Part A*, 2015, **140**, 534–543.

38 K. Laatikainen, D. Udomsap, H. Siren, H. Brisset, T. Sainio and C. Branger, Effect of template ion–ligand complex stoichiometry on selectivity of ion-imprinted polymers, *Talanta*, 2015, **134**, 538–545.